Control of domain wall pinning by localised focused Ga + ion irradiation on Au capped NiFe nanowires

D. M. Burn, and D. Atkinson

Citation: Journal of Applied Physics **116**, 163901 (2014); doi: 10.1063/1.4900437
View online: https://doi.org/10.1063/1.4900437
View Table of Contents: http://aip.scitation.org/toc/jap/116/16
Published by the American Institute of Physics

JOURNAL OF APPLIED PHYSICS **116**, 163901 (2014)

Control of domain wall pinning by localised focused Ga $^+$ ion irradiation on Au capped NiFe nanowires

D. M. Burn[a] and D. Atkinson
Department of Physics, Durham University, Durham, United Kingdom

(Received 31 July 2014; accepted 14 October 2014; published online 22 October 2014)

Understanding domain wall pinning and propagation in nanowires are important for future spintronics and nanoparticle manipulation technologies. Here, the effects of microscopic local modification of the magnetic properties, induced by focused-ion-beam intermixing, in NiFe/Au bilayer nanowires on the pinning behavior of domain walls was investigated. The effects of irradiation dose and the length of the irradiated features were investigated experimentally. The results are considered in the context of detailed quasi-static micromagnetic simulations, where the ion-induced modification was represented as a local reduction of the saturation magnetization. Simulations show that domain wall pinning behavior depends on the magnitude of the magnetization change, the length of the modified region, and the domain wall structure. Comparative analysis indicates that reduced saturation magnetisation is not solely responsible for the experimentally observed pinning behavior. © *2014 AIP Publishing LLC*. [http://dx.doi.org/10.1063/1.4900437]

I. INTRODUCTION

The behavior of domain walls (DWs) is fundamental to the process of magnetisation reversal in ferromagnetic nanowire structures. Significant interest in this area also comes from the applications potential for logic[1] and memory[2,3] and the ability to detect[4] and manipulate[5–8] magnetic nanoparticles and even cold atoms.[9] Controlling the location of biologically or chemically functionalised magnetic nanoparticles opens avenues for many areas of research, including drug delivery, nanofabrication, molecular detection, nanofluidics, and biomechanics.

DWs can propagate with magnetic field along straight nanowires,[10,11] around corners,[12,13] and can be directed along selected pathways at junctions.[7,14] The propagation field[15] and domain wall velocity[11,16] can be controlled by structural modulation of the nanowire geometry and the inclusion of features, such as constrictions[17–19] and notches,[20–22] along the wire introduce artificial DW pinning sites. Micromagnetic modelling can provide an understanding of the physical spin structure of the DWs, and has shown different DW structures depending on the nanowire geometry.[23] Furthermore, the sense of the spin rotation, or chirality, of the DW spin structure has been shown to influence DW interactions with notches.[24,25] Longitudinally asymmetrical structuring[26,27] even allows for the design of energy landscapes that present different DW energy gradients dependent upon the propagation direction of the DW, producing diode like behavior which in combination can lead to a ratchet-like system.[28–30]

Thus, lithographically defined structural features provide a wide range of parameters for controlling the propagation and pinning of domain walls in nanowires with in-plane magnetization. However, such lithographic processes present issues of scalability when moving to smaller structures and also the details of the DW interactions are sensitive to small-scale defects or variations within the lithographic features that may affect the reliability of device performance. Therefore, additional modes of control are sought which may avoid these issues and complement geometrical structuring for the control of DW processes.

Here, nanoscale localised ion-irradiation of magnetic nanowires with in-plane magnetization is investigated as a complementary method to control DW behavior. Ion beam irradiation is a well established technique for changing perpendicular magnetic anisotropy (PMA) materials such as Co/Pt where irradiation modifies the strong interfacial contribution to the anisotropy.[31] For materials with in-plane anisotropy, such as permalloy, changes in the magnetic properties are typically found at higher doses due to the damaging effects of the irradiation, which lead to a degradation in the magnetic properties for the near-surface region[32] that eventually undergoes a ferromagnetic to paramagnetic transition.[33–36]

However, irradiation induced mixing at an interface with a non-magnetic (NM) capping layer offers a lower dose approach where dose dependent modification of the magnetic properties of the material occurs before damaging effects become significant.[37]

In this study, the pinning of domain walls by localised regions with modified magnetic properties introduced by focused ion-beam irradiation in NiFe/Au nanowires was investigated experimentally. The analysis of this experimental study was supported by an investigation using quasi-static micromagnetic simulations of DW pinning associated with a region with a local reduction of the saturation magnetization, in order to determine if this is the mechanism responsible for the experimentally observed irradiation induced pinning behavior.

II. EXPERIMENTAL AND MICROMAGNETIC SIMULATION DETAILS

Individual planar nanowires were patterned on thermally oxidized silicon substrates using electron beam lithography and fabricated by thermal evaporation followed by lift-off.

[a]d.burn@imperial.ac.uk. Present address: Department of Physics, Imperial College London, London, United Kingdom.

Bilayer thin-film structures composed of 15 nm NiFe, evaporated from a single alloy source of nominal composition $Ni_{81}Fe_{19}$, followed by a 2.5 nm Au cap were deposited without breaking the vacuum. Deposition rates and thicknesses were monitored with an *in-situ* quartz rate monitor that was previously calibrated by x-ray reflectivity measurements. The nanowire structures were 400 nm wide and 100 μm long and included a 4 μm long, 2 μm wide domain wall *nucleation pad* at one end of the structure, and a 4 μm long tapered point at the other end to control DW nucleation. This structure constrained the reversal to begin from the nucleation pad in each field cycle, as the pad reverses at a lower field and the associated domain wall was injected into the nanowire.

The nanowires were modified locally by controlled exposure to focussed Ga^+ ion-beam irradiation using an FEI Helios Nanolab 600 Dual Beam system. This irradiation induced localised modifications to the bilayer structure in exposure windows positioned 25 μm apart along the length of the nanowire. These regions ranged in length from 500 nm to 5 μm along the wire axis and were exposed by rastering the beam orthogonal to the nanowire axis. Irradiation was performed at normal incidence with 30 keV Ga^+ ions using a beam current of 29 pA. Doses up to 7.6×10^{15} Ga^+/cm^2 were achieved by multiple exposures with a dwell time of 1 μs. The ion beam has a Gaussian profile and beam diameter at this current was sub-100 nm in diameter.

The magnetization reversal behavior of the nanowires was investigated using focused longitudinal magneto-optical Kerr effect (MOKE) measurements. These measurements probed the magnetization reversal behavior using a $\approx$10 μm laser spot projected onto the sample giving spatial resolution of this order. Measurements were taken as a function of position along the length of each nanowire allowing any changes to the DW propagation associated with the irradiated regions to be investigated. Magnetization reversal was driven with a 27 Hz sinusoidal magnetic field of amplitude $\pm$260 Oe along the axis of the nanowire, and the Kerr signal was averaged over many hundreds of field cycles for $\approx$2 min for each hysteresis loop.

The experimental results are supported by quasi-static micromagnetic simulations that were performed using OOMMF.[38] This analysis shows the effect of the introduction of a region of reduced M_S on 10 nm thick permalloy wires with widths from 150 nm up to 400 nm. The simulations used a $5 \times 5 \times 10$ nm mesh and typical micromagnetic parameters for permalloy, i.e., saturation magnetization, $M_S = 860 \times 10^3$ A/m, exchange, $A = 13 \times 10^{-12}$ J/m and zero magnetocrystalline anisotropy.[25] A high value for the damping parameter of $\alpha = 0.5$ was used to reduce computational time and is justified here because the simulations were performed in a quasi-static regime.[39] Simulations were performed with 1 μm or 2 μm long simulation windows, where the magnetostatic effects associated with the abrupt ends of the nanowire were corrected for with fixed spins at the nanowire ends.[40] Simulations were initiated with an initial DW structure in the center of a region of reduced M_S representing the irradiated region and an axial field was applied in 1 Oe steps until the DW structure de-pinned from the reduced-M_S region and propagated freely along the nanowire.

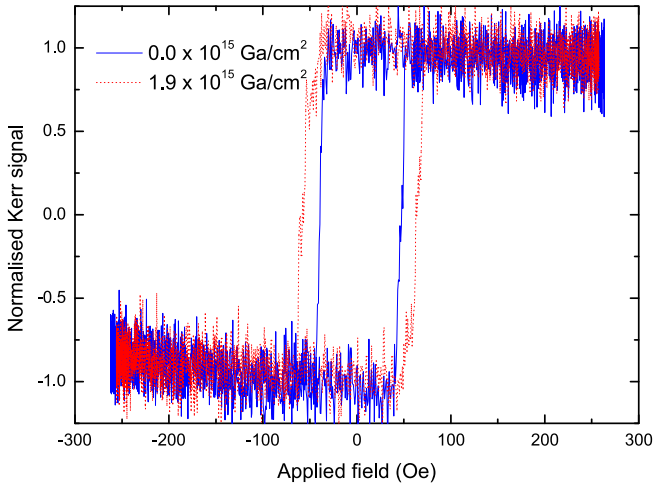

FIG. 1. MOKE hysteresis loops from a 400 nm wide, 15 nm NiFe/2.5 nm Au nanowire. The loops are measured either side of a 2 μm wide region irradiated with a dose of 1.9×10^{15} Ga/cm^2.

III. RESULTS AND DISCUSSION

Focussed MOKE measurements on the nanowires gave hysteresis loops demonstrating the reversal behavior of the wires. An example is shown in Figure 1 for measurements at two locations along the length of a nanowire, either side of a 2 μm wide region irradiated with a dose of 1.9×10^{15} Ga^+/cm^2. A significant difference in the coercivity was observed and further subtle changes to the sharpness of the loops were also apparent in the reversal behavior measured at positions before and after the irradiated region.

The magnetisation reversal field was determined from the hysteresis loops recorded at different positions along the length of wires that included multiple irradiated regions. Figure 2 shows discrete step-like increases in the reversal field that occur at the position of the irradiated regions, separated by sections with a constant reversal field.

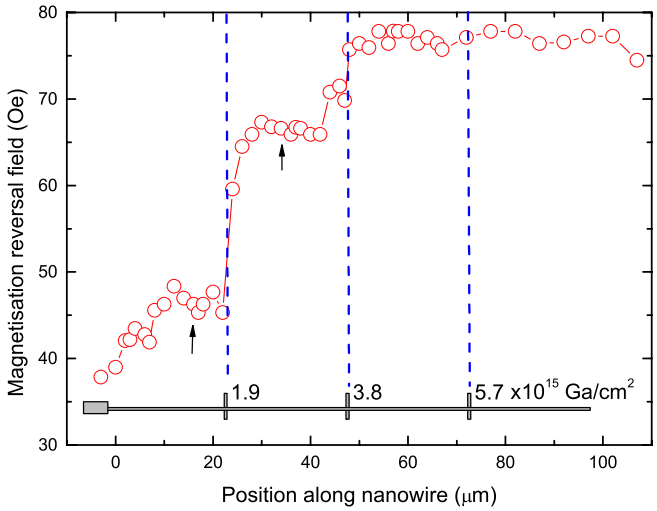

FIG. 2. Magnetisation reversal field as a function of measurement position along a 400 nm wide NiFe/Au nanowire. The schematic of the nanowire shows the locations of the 2 μm wide irradiated regions with increasing dose and with 25 μm separation. The arrows mark the position of the hysteresis loops in Figure 1.

This behavior is explained by the injection and propagation of a DW initiated from the nucleation pad end of the wire. The DW propagates freely at a relatively low, constant field of about 45 Oe along the un-irradiated section of the nanowire. The DW becomes pinned at the irradiated region and a higher field is then required to de-pin the DW before it can continue to propagate in the remaining length of the un-irradiated nanowire. At the first irradiated region a reversal field of 67 Oe was required for the DW to overcome the de-pinning field associated with this modified region. A further increase in field up to 77 Oe was required to de-pin the DW from the next irradiated region that has a higher dose of 3.8×10^{15} Ga^+/cm^2.

The DW de-pinning field was determined for a range of irradiation doses with a 2 μm long irradiated region. The results are shown in Figure 3 as a function of irradiation dose and also as a function of the effective saturation magnetization, M_S, of the irradiated region. The estimates of M_S are based on previous magnetic characterisation of the irradiation on micro-scale bilayer structures.[37] The reversal field increases with irradiation dose, and decreases linearly with reduction in the estimated magnetization, M_S, of the pinning site, suggesting an increased DW pinning effect as the local saturation magnetisation of the irradiated region is reduced. This linear trend is offset from zero by 44 ± 6 Oe for the un-irradiated sample ($M_S = 860 \times 10^3$ A/m). This offset represents the field required for magnetisation reversal in the un-irradiated wire and is indicative of the field required to inject a DW from the nucleation pad into the nanowire. It is anticipated that DWs would propagate at a lower field in the un-irradiated wire if the DWs were introduced by some other method, such as with a localised pulsed-field.[15]

The DW pinning behavior was also investigated as a function of the length of the irradiated region using a constant dose of 7.6×10^{15} Ga^+/cm^2, see Figure 4. For this

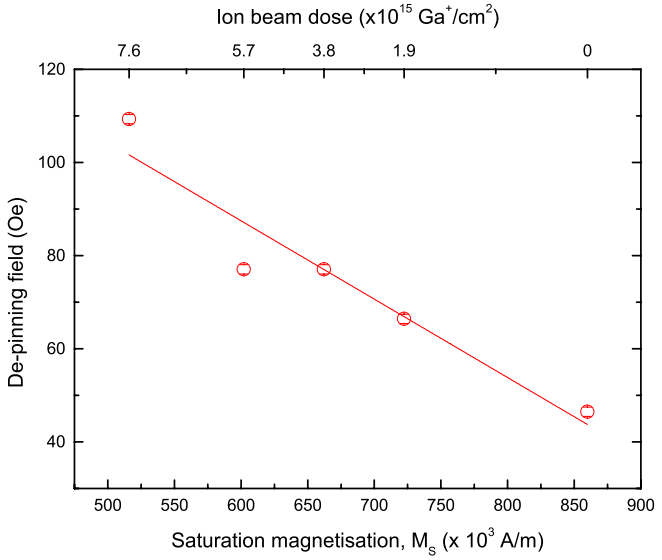

FIG. 3. DW de-pinning field as a function of the ion dose and the estimated saturation magnetisation for 2 μm wide irradiated regions along a 400 nm wide NiFe/Au nanowire. The saturation magnetisation is found from the irradiation dose based on previous work.[37] The errors are comparable with the data points and the straight line is a best fit to the data.

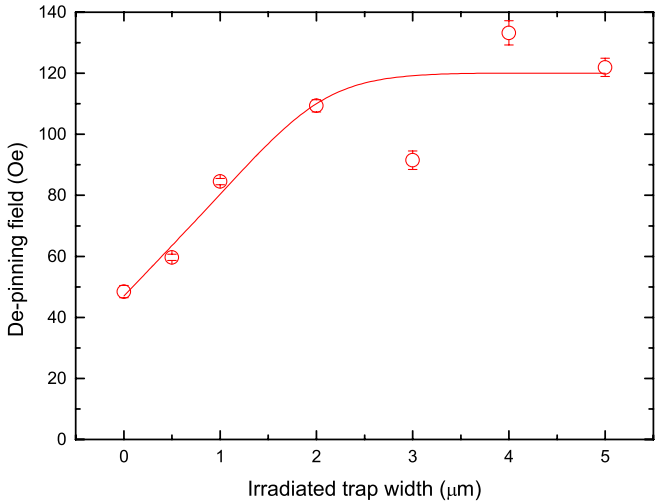

FIG. 4. DW de-pinning field as a function of the width of an irradiated region (7.6×10^{15} Ga/cm^2) along a 400 nm wide NiFe/Au nanowire. The errors are comparable with the data points and the line is a guide to the eye.

bilayer system, this dose corresponds to a reduction of the saturation magnetization to an approximate value of $M_S = 520 \times 10^3$ A/m. The de-pinning field increases with increasing length of irradiated region up to approximately 2 μm and beyond which the irradiated region has little further effect upon the de-pinning field. Again, these results also show a ~45 Oe offset of the de-pinning field with no irradiation, which is attributed to the field required for injection of the DW from the nucleation pad into the nanowire.

In addition to the experimental measurements, quasi-static micromagnetic simulations have been performed to give insight into the physical processes taking place when a DW interacts with a region of reduced M_S. Figure 5 shows the de-pinning field of a DW as a function of saturation magnetization for different wire widths and for both vortex and transverse domain wall structures. In all cases, the de-pinning field increases linearly with a reduction in M_S in the

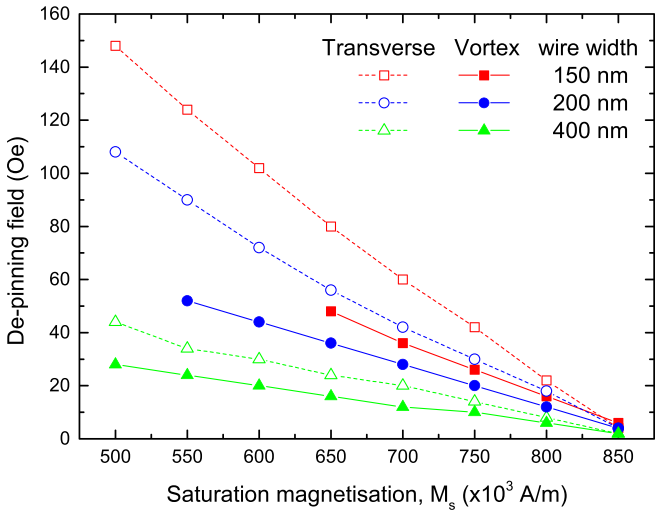

FIG. 5. DW de-pinning field from micromagnetic simulations of a 200 nm wide region as a function of saturation magnetization, M_S. The behavior is shown for both transverse and vortex domain wall structures in various width wires and the lines are guides to the eye.

localised region. Comparing the nanowire geometries, the simulations show stronger pinning is found for narrower wires and that the transverse wall structures are more heavily pinned than the vortex structures. For the lower M_S values, the vortex structure becomes unstable in the narrower wires and transitions into a transverse DW. In these cases, the vortex wall data are omitted.

The linear trend in de-pinning field was also observed in the experimental measurements, although the length of the pinning site was much larger. Furthermore, comparing the simulations and experimental results for the 400 nm wide wire shows differences in the pinning field amplitude, with lower pinning fields observed in the simulations. Some of this difference may be attributed to the different thicknesses of 15 nm and 10 nm, respectively, studied in the experiments and simulations.[41]

Here, the trends in the de-pinning field have been investigated using micromagnetic simulations. The aim was to investigate the idea that the irradiated region of the nanowire with modified magnetic properties near the interface could be represented by a simplistic model based on an equivalent region with a reduced value of the M_S. Again the DW reversal behavior was compared for different nanowire widths and both transverse and vortex domain wall structures. Figure 6 shows the de-pinning field as a function of the length of the region with reduced M_S (500×10^3A/m). For transverse walls in narrower wires, the pinning field initially increases rapidly with increasing length of the pinning region and then approaches a plateau. For the 400 nm wide wire, the de-pinning field shows a more gradual increase. In all cases, the transverse walls are pinned more strongly than the vortex walls, and the vortex structure is again transformed to a transverse wall in the narrower wires as the length of the pinning region is increased.

The trend observed in the micromagnetic data have a similar form to that observed for the measured pinning field as a function of the length of the irradiated region, with an initial rapid rise in the pinning field followed by a levelling-off

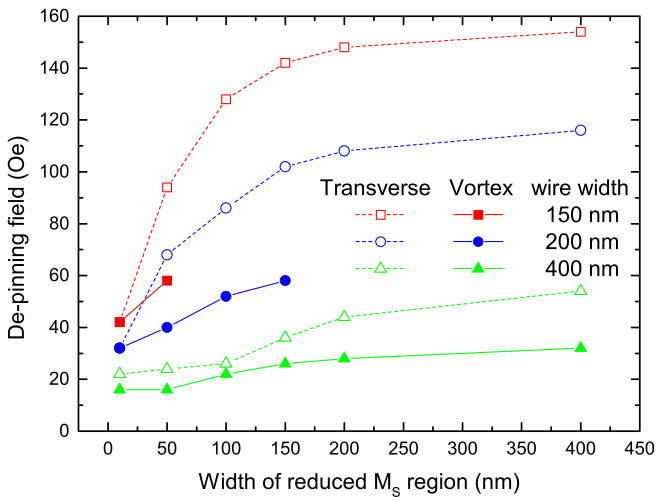

FIG. 6. DW de-pinning field from micromagnetic simulations as a function of the width of a region of reduced M_S ($M_S = 500 \times 10^3$ A/m). The behavior is shown for both transverse and vortex domain wall structures in various width wires and the lines are guides to the eye.

of the pinning strength for longer pinning regions. However, the length-scale of the pinning region in the experimental data was significantly larger.

The general trend of pinning with increasing size of the pinning site structure has been explained previously by theoretical modelling of DW pinning at defects where the pinning potential increases with the size of the defect, until the defect is larger than the domain wall size.[42] For DWs in planar nanowires, the wall length along the nanowire is comparable with the width of the nanowire. The pinning behavior as a function of the length of the pinning feature obtained from the micromagnetic simulations follows this pinning model with the pinning strength increasing rapidly until the length of the pinning feature is comparable with the width of the wire and thus the wall length. The experimental pinning behavior shows a linear increase of the de-pinning field with pinning site length up to 2 μm followed by little further changes in the de-pinning field for longer pinning features. The general trend is qualitatively similar to the micromagnetic analysis but the pinning features are an order of magnitude longer in the experimental work.

Overall, whilst the micromagnetic modeling of pinning based simply on a localised reduction of the saturation magnetization indicates a route to DW pinning, this mechanism does not provide a complete explanation for the pinning behavior observed experimentally for the ion-beam induced DW pinning in the NiFe/Au bilayer nanowires studied here. The experimentally observed pinning is stronger and varies over a longer length-scale than that predicted from the quasi-static micromagnetic simulations. Any intrinsic pinning due to edge roughness and experimental defects are not accounted for by the perfect structures simulated nor are the finite temperature in the experiments or differences between the material parameters. Therefore, although the saturation magnetization is reduced by the ion-beam irradiation, other factors are modified and may also be involved.[37] It has been observed previously that interfacial intermixing at the NiFe/Au interface increases with increasing ion dose and here this may contribute to the increased DW pinning, although the topological roughness is not significantly enhanced. Also, the magnetic damping has also been shown to increase with ion-beam irradiation[43] and this may have an effect on the dynamic interaction of a propagating DW with the pinning region in our experimental measurements. This dynamic behavior was not included in the quasi-static micromagnetic analysis performed here with an artificially high damping parameter of $\alpha = 0.5$.[39]

Nonetheless, the micromagnetic simulations are informative and further analysis gives insight into the interactions taking place between the DW spin structure and the regions of reduced M_S of the nanowire which leads to the pinning. The DW structure of both transverse and vortex DWs are shown in Figure 7 for different length regions of reduced M_S (750×10^3 A/m). These micromagnetic structures occur at a field just below the de-pinning field for that pinning region. For transverse walls, a larger proportion of the DW resides within the reduced M_S region as the trap length increases and this lead to a stronger pinning effect. In contrast, for the vortex walls only the trailing edge of the DW appears to be

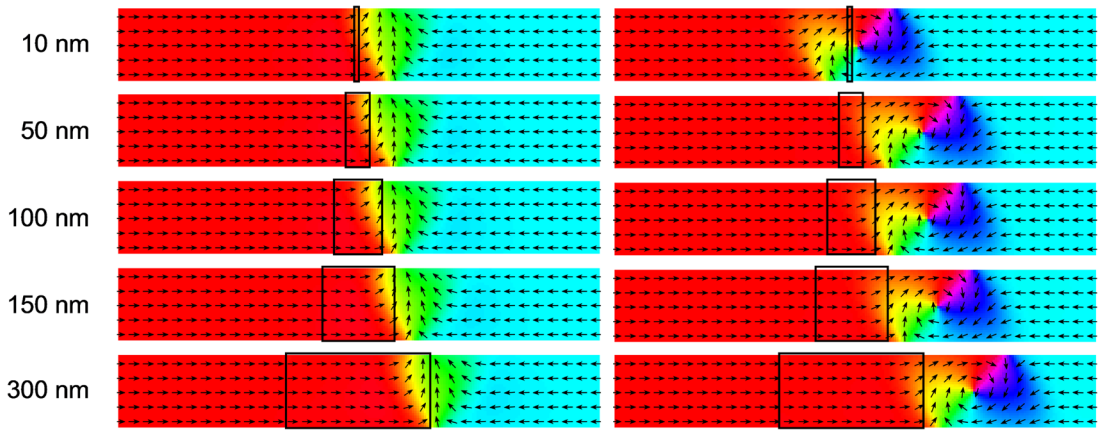

FIG. 7. Micromagnetic simulations of domain wall spin structure in 10 nm thick, 150 nm wide planar nanowires. Dws pinned by a region of reduced $M_S = 750 \times 10^3$ A/m of various length indicated by the black outline box. The simulations show the micromagnetic structure at a field directed to the right with a magnitude just below the de-pinning field.

pinned on the edge of the reduced M_S region, leaving the majority of the wall structure to reside outside of the reduced M_S region. However, for the 10 nm wide region the centre of the vortex DW is pinned by the low M_s region, again showing more complex behavior.

IV. CONCLUSIONS

Highly localised regions of Ga^+ irradiation have been used to modify the magnetic properties of NiFe/Au bilayer in order to create pinning sites for domain walls in planar nanowires. Intermixing of the Au and NiFe at the interface modifies the magnetic properties locally. One aspect of this is a reduction of the saturation magnetisation, M_S. Experimentally DWs become pinned by these modified regions during their propagation along the nanowires, requiring a higher field to de-pin and continue their propagation. The de-pinning field increases with increasing irradiation dose and the de-pinning field also shows a dependence upon the length of the irradiated region, initially increasing with the length of the pinning region before levelling out for longer irradiated regions.

Micromagnetic simulations show pinning behavior as a function of pinning site length and reduced M_S that was found to be qualitatively similar to the experimental results. However, this micromagnetic modeling does not provide a direct explanation for the pinning behavior observed experimentally for the ion-beam induced DW pinning behavior in the NiFe/Au bilayer nanowires, other factors including increased interfacial intermixing and enhanced damping may also play a role. The micromagnetic simulations do, however, give further insight into the effect of the DW structure on the pinning mechanisms for a domain wall encountering a localised region of reduced saturation magnetization.

This work shows localised selective pinning of DW structures can be achieved through control of the geometry of focus-ion-beam irradiated regions in NiFe/Au bilayer nanowires. Control over the pinning associated with the DW structure may provide a useful approach for devices physics involving the manipulation of magnetic DWs.

[1]D. A. Allwood, G. Xiong, C. C. Faulkner, D. Atkinson, D. Petit, and R. P. Cowburn, Science **309**, 1688 (2005).
[2]S. S. P. Parkin, M. Hayashi, and L. Thomas, Science **320**, 190 (2008).
[3]D. S. Eastwood, L. K. Bogart, and D. Atkinson, Acta Phys. Pol. **118**, 719 (2010).
[4]P. Vavassori, V. Metlushko, B. Ilic, M. Gobbi, M. Donolato, M. Cantoni, and R. Bertacco, Appl. Phys. Lett. **93**, 203502 (2008).
[5]M. Donolato, P. Vavassori, M. Gobbi, M. Deryabina, M. F. Hansen, V. Metlushko, B. Ilic, M. Cantoni, D. Petti, S. Brivio, and R. Bertacco, Adv. Mater. **22**, 2706 (2010).
[6]E. Rapoport and G. S. D. Beach, Appl. Phys. Lett. **100**, 082401 (2012).
[7]G. Ruan, G. Vieira, T. Henighan, A. Chen, D. Thakur, R. Sooryakumar, and J. O. Winter, Nano Lett. **10**, 2220 (2010).
[8]A. Torti, V. Mondiali, A. Cattoni, M. Donolato, E. Albisetti, A. M. Haghiri-Gosnet, P. Vavassori, and R. Bertacco, Appl. Phys. Lett. **101**, 142405 (2012).
[9]A. D. West, K. J. Weatherill, T. J. Hayward, P. W. Fry, T. Schrefl, M. R. J. Gibbs, C. S. Adams, D. A. Allwood, and I. G. Hughes, Nano Lett. **12**, 4065 (2012).
[10]R. P. Cowburn, D. A. Allwood, G. Xiong, and M. D. Cooke, J. Appl. Phys. **91**, 6949 (2002).
[11]D. Atkinson, D. A. Allwood, G. Xiong, M. D. Cooke, C. C. Faulkner, and R. P. Cowburn, Nat. Mater. **2**, 85 (2003).
[12]D. A. Allwood, G. Xiong, M. D. Cooke, C. C. Faulkner, D. Atkinson, N. Vernier, and R. P. Cowburn, Science **296**, 2003 (2002).
[13]N. Vernier, D. A. Allwood, D. Atkinson, M. D. Cooke, and R. P. Cowburn, Europhys. Lett. **65**, 526 (2004).
[14]C. C. Faulkner, D. A. Allwood, M. D. Cooke, G. Xiong, D. Atkinson, and R. P. Cowburn, IEEE Transactions on Magnetics. **39**, 2860 (2003).
[15]D. M. Burn, E. Arac, and D. Atkinson, Phys. Rev. B **88**, 104422 (2013).
[16]D. M. Burn and D. Atkinson, Appl. Phys. Lett. **102**, 242414 (2013).
[17]Y. Yokoyama, Y. Suzuki, S. Yuasa, K. Ando, K. Shigeto, T. Shinjo, P. Gogol, J. Miltat, A. Thiaville, T. Ono, and T. Kawagoe, J. Appl. Phys. **87**, 5618 (2000).
[18]D. Lacour, J. A. Katine, L. Folks, T. Block, J. R. Childress, and M. J. Carey, Appl. Phys. Lett. **84**, 1910 (2004)
[19]A. Himeno, T. Ono, S. Nasu, K. Shigeto, K. Mibu, and T. Shinjo, J. Appl. Phys. **93**, 8430 (2003).
[20]C. C. Faulkner, M. D. Cooke, D. A. Allwood, D. Petit, D. Atkinson, and R. P. Cowburn, J. Appl. Phys. **95**, 6717 (2004).
[21]G. S. D. Beach, J. Magn. Magn. Mater. **320**, 1272 (2008).
[22]L. K. Bogart, D. S. Eastwood, and D. Atkinson, J. Appl. Phys. **104**, 033904 (2008).
[23]Y. Nakatani, A. Thiaville, and J. Miltat, J. Magn. Magn. Mater. **290–291**, 750 (2005).

[24]D. Atkinson, D. S. Eastwood, and L. K. Bogart, Appl. Phys. Lett. **92**, 022510 (2008).
[25]L. K. Bogart, D. Atkinson, K. O'Shea, D. McGrouther, and S. McVitie, Phys. Rev. B **79**, 054414 (2009).
[26]D. A. Allwood, G. Xiong, and R. P. Cowburn, Appl. Phys. Lett. **85**, 2848 (2004).
[27]M. T. Bryan, T. Schrefl, and D. A. Allwood, Appl. Phys. Lett. **91**, 142502 (2007).
[28]A. Himeno, S. Kasai, and T. Ono, Appl. Phys. Lett. **87**, 243108 (2005).
[29]H. G. Piao, H. Lee, and J. Yoon, IEEE Trans. Magn. **46**, 1844 (2010).
[30]A. Himeno, T. Okuno, S. Kasai, T. Ono, S. Nasu, K. Mibu, and T. Shinjo, J. Appl. Phys. **97**, 066101 (2005).
[31]C. Chappert, H. Bernas, J. Ferré, V. Kottler, J. P. Jamet, Y. Chen, E. Cambril, T. Devolder, F. Rousseaux, V. Mathet, and H. Launois, Science **280**, 1919 (1998).
[32]C. M. Park and J. A. Bain, J. Appl. Phys. **91**, 6830 (2002).
[33]C. C. Faulkner, D. Atkinson, D. A. Allwood, and R. P. Cowburn, J. Magn. Magn. Mater. **319**, 9 (2007).
[34]C. M. Park and J. A. Bain, IEEE Trans. Magn. **38**, 2237 (2002).
[35]J. Fassbender and J. McCord, Appl. Phys. Lett. **88**, 252501 (2006).
[36]W. M. Kaminsky, G. A. C. Jones, N. K. Patel, W. E. Booij, M. G. Blamire, S. M. Gardiner, Y. B. Xu, and J. A. C. Bland, Appl. Phys. Lett. **78**, 1589 (2001).
[37]D. M. Burn, T. P. A. Hase, and D. Atkinson, J. Phys.: Condens. Matter **26**, 236002 (2014).
[38]See http://math.nist.gov/oommf for the OOMMF code.
[39]J. Fidler, J. Phys. D: Appl. Phys. **33**, R135 (2000).
[40]R. D. McMichael and M. J. Donahue, IEEE Trans. Magn. **33**, 4167 (1997).
[41]K. J. Kirk, J. N. Chapman, and C. D. W. Wilkinson, J. Appl. Phys. **85**, 5237 (1999).
[42]R. C. O'Handley, *Modern Magnetic Materials Principles and Applications* (Wiley, 2000).
[43]J. King, A. Ganguly, D. M. Burn, S. Pal, E. A. Sallabank, T. P. A. Hase, A. T. Hindmarch, A. Barman, and D. Atkinson, Appl. Phys. Lett. **104**, 242410 (2014).